Steel and Composite Structures, *Vol. 15, No. 5 (2013) 539-566*
DOI: http://dx.doi.org/10.12989/scs.2013.15.5.539

Modelling aspects of the seismic response of steel concentric braced frames

M. D'Aniello *, G. La Manna Ambrosino [a], F. Portioli [b] and R. Landolfo [c]

Department of Structures for Engineering and Architecture, University of Naples "Federico II", Via Forno Vecchio 36, 80134 Naples, Italy

(*Received December 15, 2012, Revised June 14, 2013, Accepted August 05, 2013*)

Abstract. This paper summarises the results of a numerical study on the non linear response of steel concentric braced frames under monotonic and cyclic loads, using force-based finite elements with section fibre discretisation. The first part of the study is addressed to analyse the single brace response. A parametric analysis was carried out and discussed to evaluate the accuracy of the model, examining the influence of the initial camber, the material modelling, the type of force-based element, the number of integration points and the number of fibers. The second part of the paper is concerned with the modelling issues of whole braced structures. The effectiveness of the modelling approach is verified against the nonlinear static and dynamic behaviour of different type of bracing configurations. The model sensitivity to brace-to-brace interaction and the capability of the model to mimic the response of complex bracing systems is analyzed. The influence of different approaches for modelling the inertia, the equivalent viscous damping and the brace hysteretic response on the overall structural response are also investigated. Finally, on the basis of the performed numerical study general modelling recommendations are proposed.

Keywords: steel concentric bracing; buckling; cyclic response; numerical modelling; seismic analysis

1. Introduction

In conventional concentrically braced steel frames the seismic performance is primarily dependent on the behaviour of the bracing elements, which are the members devoted to dissipate the input energy according to the philosophy of capacity design implemented in current codes. As it is well known, differently from eccentric bracing and buckling restrained braces (D'Aniello *et al*. 2006a, b, 2008, Mazzolani *et al*. 2009, Della Corte *et al*. 2013) where the bracing elements do not show overall buckling, the hysteretic behaviour of steel concentric braces is characterized by the buckling in compression, the yielding in tension, moderate hardening and significant pinching when the deformation reverses. As a matter of fact this nonlinear performance is very complex to be simulated. On the other hand, an accurate model for braces is essential for an effective estimation of both interstorey drift ratios and ductility demand of concentrically braced frames

*Corresponding author, Assistant Professor, E-mail: mdaniel@unina.it
[a] Ph.D. Student, E-mail: giuseppe.lamannaambrosino@unina.it
[b] Assistant Professor, E-mail: fportiol@unina.it
[c] Full Professor, Head of Department, E-mail: landolfo@unina.it

http://www.techno-press.org/?journal=scs&subpage=8 ISSN: 1229-9367 (Print), 1598-6233 (Online)

under seismic conditions.

In general, the hysteretic models used to simulate the brace nonlinear response introduce significant simplifications if compared to the experimental behaviour. These simplifications could lead to incorrect prediction of the peak responses or even behaviour modes. The hysteretic behaviour of steel concentric braces has been experimentally and theoretically investigated by a number of authors in the last thirty years (Jain and Goel 1978, Black *et al*. 1980, Shibata 1982, Ikeda and Mahin 1986, Tremblay 2002, Uriz 2005, Goggins *et al*. 2006, 2008, Dicleli and Mehta 2007, Dicleli and Calik 2008, Lee and Noh 2010). In particular, three different modelling approaches may be recognized (Uriz *et al*. 2008): (i) phenomenological models (PM); (ii) continuum finite element models (FEM); (iii) physical-theory models (PTM).

PMs are based on equivalent one-dimensional truss elements with hysteretic behaviour simulating the experimental response (Jain and Goel 1978, Ikeda and Mahin 1986). The hysteretic properties are defined using a set of empirical rules for the shape of hysteretic loops without representing the physical phenomena (e.g., the out-of-plane displacement induced by buckling) that characterize the brace response. Although this approach allows simulating the overall behaviour of such braces, there are some disadvantages limiting their effective use.

Indeed, the reliability and accuracy of these models depend on the availability of experimental data, which are necessary to determine the appropriate modelling parameters. Moreover, these models do not provide any information on damage produced by the lateral buckling of braces. Hence, in performance-based assessment it is not possible to evaluate the lateral displacements which can damage non-structural elements and interfere with the operation of adjacent mechanical components, such as elevators.

Contrary to PMs, FEM is the most accurate approach to simulate the brace behaviour. Indeed, general purpose finite element programs capable of large displacement analysis allow to overcome the modelling limitations previously illustrated. In FEM approach braces and their connections can be simulated using shell or solid elements characterized by appropriate material models. Several studies of this type have been carried out recently (Fell *et al*. 2009, Takeuchi and Matsui 2011, Serra *et al*. 2012). However, because of the huge time amount requested for the preparation of input files and for calculations, such detailed finite element models can be mainly used to simulate local details. Being the application to seismic analysis of whole building frame very difficult, FE models are not convenient for structural engineering practice and even research in seismic assessment of whole structures.

In PTM approach the brace hysteretic behaviour is usually modelled with two elements connected by a generalized plastic hinge for braces simply pinned. Inelastic hinges concentrated at the element ends and mid-span are used in the case of fixed-end braces (Jin and El-Tawil 2003, Uriz *et al*. 2008). In this type of models geometric nonlinearities (namely an initial camber) are usually introduced to account for buckling of braces.

PTMs can generally overcome the disadvantages and the application limits of PMs and FEMs. The main advantage of PTMs consists in the number of experimental parameters to be specified, which is less than the case of PMs. The basic input data to be implemented are the material properties, the brace geometry and the distribution of fibers at critical sections. Moreover, although PTMs need a computational effort increased respect to PMs, the complexity in preparing input files and the computational time expense typically necessary in FEMs are overcome. Only few factors are not taken into account as initial stresses and variations of the shape of the cross section due to local/distortional buckling.

A large number of research studies on the application of PTMs for pushover and time history

analyses of various bracing shapes and configurations can be found in the literature (e.g., Dicleli and Mehta 2007, Dicleli and Calik 2008, Uriz 2005, Wijesundara 2009, Goggins and Salawdeh 2012, Salawdeh and Goggins 2013).

In these studies different modelling assumptions are used, including the initial camber (e.g., camber amplitude obtained by means of analytical formulations or simply assumed as a fixed percentage of the brace total length), the material model (e.g., monotonic and hysteretic) and the type of inelasticity element (e.g., distributed and concentrated plasticity).

It is known that the modelling of buckling, post-buckling and cyclic behaviour of braces is sensitive to these parameters, which have been set differently among the literature studies.

As a consequence, it is interesting to verify the accuracy and the suitability of the existing formulations in predicting the monotonic and cyclic response of braced structures under static and dynamic loading conditions. To this aim, in the present paper the comparison of the response which can be obtained for the formulations proposed in the literature has been carried out, extending the analysis to structural configurations and loading conditions different from those used for validation in the relevant original studies.

In the opinion of Authors, this comparison is a key issue for the numerical simulation using PTMs, considering that this type of models have been used to perform numerical analyses devoted to determine the ductility demand and design parameters, such as the behaviour factors, the post-buckling strength of brace in compression for capacity design and overall over-strength. On the other hand, being nonlinear analyses introduced in modern seismic codes, nowadays apart from researchers it is fundamental to provide adequate numerical modelling instructions also to FE analysts (D'Aniello *et al*. 2010), because the accuracy and effectiveness of numerical models strongly influence the assessment of demands imposed on structural elements and the global ductility demands, as well.

These concerns motivated the study presented herein, which is also addressed at providing recommendations for modelling of conventional concentric braced frames within the context of a specific computational platform, by examining the capability of handling different geometries as well as material and geometric nonlinearities. Besides, it should be noted that some phenomena such as the plastic local buckling and the low-cycle fatigue effects were not considered in this study. Indeed, fibre PTMs do not allow accounting for local buckling and computing the actual local distribution and the amplitude of strains in the plastified zones due to local nonlinear geometric effects. Although the former aspect cannot be accounted for in PTMs, as early demonstrated by Uriz *et al*. (2008) the plastic local buckling is poorly significant on the overall hysteretic force-displacement response of braces made of compact sections, as those examined in the present study and generally adopted in seismic design according to modern codes (e.g., EN1998-1). For what concerns the evaluation of low-cycle fatigue capacity of braces, it is known that this aspect is physically dependent on the accumulation of damage, namely the strains. This implies that, using such a kind of modelling strategy, it could be convenient to verify a-posteriori the fracture life of braces by means of refined analytical equations proposed by a number of researchers (Lee and Goel 1987, Tang and Goel 1989, Archambault *et al*. 1995, Tremblay 2002, Shaback and Brown 2003, Tremblay *et al*. 2003) and recently updated on a large database of experimental results, thus proposing predictive expressions as function of both the global and the local slenderness of braces (Nip *et al*. 2010).

It is worth of mentioning that recent studies have proposed novel fibre elements accounting for low-cycle fatigue (Uriz 2005, Wijesundara 2009, Salawdeh and Goggins 2013), but as noted by the proposers all parameters used in the model should be calibrated to compensate the fact that

PTMs do not allow computing the actual strains. The application to low-cycle fatigue might be developed in a further study.

On the basis of the motivations previously discussed, a wide systematic study has been carried out by varying the fundamental numerical parameters at the same set of case studies, which have been selected to be representative of a wide range of structural configurations, in order to evaluate the accuracy and the suitability of the existing formulations to predict the monotonic and cyclic response of braced structures under static and dynamic loading conditions.

The paper is organized into two main parts. After a brief introduction on the basic features of the generated models, the results of the parametric analysis on single braces are presented and discussed. The effectiveness of modelling assumptions are validated against experimental results available from tests by Black *et al*. (1980). In the second part the modelling aspects of braced frames are investigated and the accuracy has been verified against experimental results on different building prototypes under pseudo-static (Wakawayashi *et al*. 1970, Yang *et al*. 2008) and dynamic (Uang and Bertero 1986) conditions.

2. Numerical model for conventional concentric bracing

The numerical models implemented in this study were generated using the nonlinear finite element based software "Seismostruct". The models were developed using the distributed inelasticity elements (e.g., Filippou and Fenves 2004, Scott and Fenves 2006, Fragiadakis and Papadrakakis 2008). These elements account for distributed inelasticity through integration of material response over the cross section and integration of the section response along the length of the element. The cross-section behaviour is reproduced by means of the fibre approach, assigning a uniaxial stress-strain relationship at each fibre.

For the use of distributed inelasticity elements it is not necessary to carry out a specific calibration of the response curve parameters, thus resulting more advantageous respect to the more common lumped-plasticity models.

Distributed inelasticity frame elements can be formulated with either displacement-based (DB) approach or the more recent force-based (FB) approach (Spacone *et al*. 1996, Calabrese *et al*. 2010). In the former case displacement shape functions are used, instead in the second approach, equilibrium is strictly imposed, namely it is perfectly dual of previous approach. In this study FB formulated elements are used. This choice is due to the fact that FB formulation can be considered as "exact" as respect to DB formulation (Calabrese *et al*. 2010), because satisfying equilibrium the force field is always exact for any level of inelastic deformation, even in the presence of strength softening (which is typically the case of buckling in steel braces).

The numerical integration method used is based on the Gauss-Lobatto distribution (Abramowitz and Stegun 1964, Szabó and Babuška 1991), which includes, at a minimum, monitoring points at each end of the element. Such feature allows each structural member to be modelled with a single FE element, thus requiring no meshing for each element. In the Gauss-Lobatto integration scheme the first and last integration points always coincide with the end sections. This is very advantageous for the case of braces because the maximum internal forces (N, M) develop at the end of the element.

Second order effects have been accounted in all analyses presented in this paper, by assuming large displacements/rotations and large independent deformations relative to the chord of the frame element through the employment of the co-rotational formulation given by Correia and Virtuoso (2006).

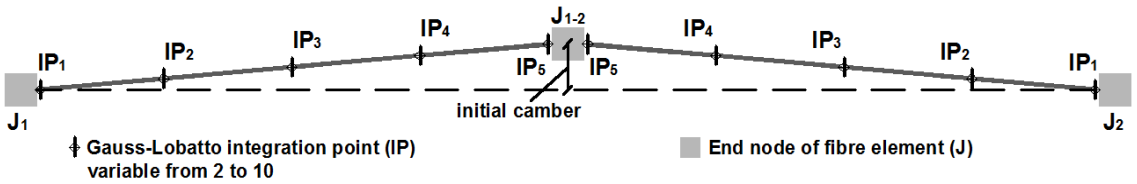

Fig. 1 The implemented model to mimic the brace behaviour

Table 1 Characteristics of the brace specimens (from Black *et al*. 1980)

Test ID	Type of section	Size	f_{ym}	L	L_s	$\lambda = kL/r$
(-)	(-)	(-)	(MPa)	(mm)	(mm)	(-)
1	W	203 × 508 × 6.4 × 10.2	278	3810	3188	120
15	CHS	113.64 × 6.02	327	3070	2448	80
17	SHS	101.60 × 101.60 × 6.35	407	3050	2428	80

In the present study, the braces were modelled with frame elements arranged to have a lateral (either bilinear or sinusoidal) shape with an initial camber (Δ_o). Indeed, the presence of this initial out-of-plane imperfection allows reproducing the transverse deformation of the brace.

Uriz *et al*. (2008) proposed to use an initial camber equal to 0.05-0.1% of the brace length applied at brace mid-span. The problem of the calculation of initial camber was differently addressed herein. Indeed, in order to reproduce the buckling response as close as possible to the experimental behaviour, the accuracy of some theoretical models was investigated, as described in Section 3.2.2 in more detail.

For monotonic and cyclic static analysis, it was applied an incremental horizontal displacement history equal to that experimentally applied during each test. In particular, the geometric nonlinearity formulation (i.e., "large displacements and small strains") was adopted and the Skyline solver was used for each displacement-step to ensure the equilibrium of the internal member forces and overall frame base shear at each iteration.

For dynamic time history analysis the numerical response was calculated using the Newmark numerical integration scheme.

Fig. 1 schematically shows the type of model investigated in this study, where integration points (IP) per element and the end joints (J) are clearly highlighted.

3. Characterization of single brace model: Parametric study

3.1 Generality

In order to characterize the response of the single brace model, the following parameters were investigated: the type of material model, the initial camber (Δ_o), the type of FB inelasticity (distributed or concentrated) elements, the number of IPs used along each of these line elements, the number of elements and shape of the initial camber, the number of fibers.

To investigate the influence of different parameters, the numerical curves were compared to the experimental tests on strut specimens indicated as No. 1, 15 and 17 in Black *et al*. (1980). For each brace specimen, Fig. 2 depicts the configuration of the specimens, while Table 1 reports the reference of the test ID, the member size, the average yield stress of the steel (f_{ym}), the total length (L), the specimen length (L_s) and the brace effective slenderness ratio ($\lambda = kL/r$).

3.2 Investigated parameters

3.2.1 Material models

The influence of two different type of steel models were investigated, namely:

(a) Menegotto-Pinto (MP) hysteretic model;
(b) Bi-linear kinematic (BLK) model.

Except for the elastic modulus (E) and the yield stress (f_y), the parameters used for the monotonic and cyclic response have been calibrated on the basis of the average stress-strain relationship derived from cyclic coupon tests performed by Black *et al*. (1980).

It is worth noting that the material library of the software used for the analysis (namely Seismostruct) implements the Menegotto and Pinto (1973) modified by Filippou *et al*. (1983) to include isotropic strain hardening. In the examined cases the parameters accounting for isotropic strain hardening have been set equal to zero, thus practically obtaining the same results of those given by the original MP formulation. This choice has been taken in order to simulate faithfully the overall force-displacement response of braces. Indeed, the experimental evidence showed that the cyclic behaviour of bracings do not appreciably experience isotropic hardening at overall level, because this material effect is counterbalanced by the deterioration due to the buckling and corresponding plastic hinging in the brace. Since PTMs cannot simulate the plastic local buckling, neglecting the isotropic component of material model allowed to fictitiously compensate this effect at global level.

In order to clarify the role of each parameters in case of MP model, the material parameters are described hereinafter as follows:

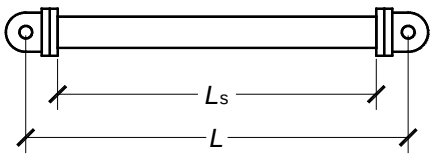

Fig. 2 Geometry of the brace specimens

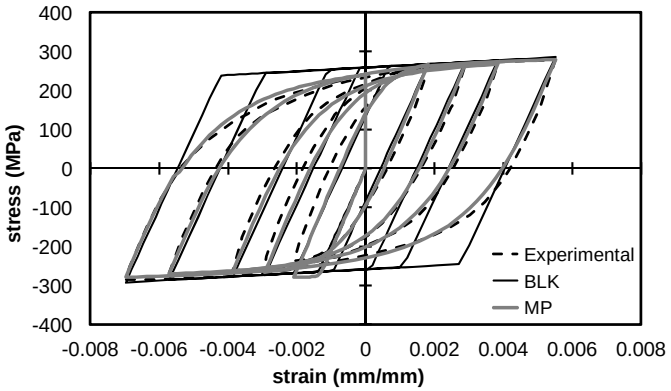

Fig. 3 Calibrated vs. Experimental steel response

Table 2 Calibrated parameters of steel hysteretic models

Steel model	E_h	R_0	A_1	A_2	A_3	A_4
MP	0.025	20.00	18.50	0.15	0.00	1.00
BLK	0.025	-	-	-	-	-

- The kinematic hardening E_h;
- The curvature parameters R_0, which characterize the shape of the transition curve between initial and post-yield stiffness allowing a representation of the Bauschinger effect;
- A_1 and A_2, which affect the shape of the hysteretic curve and hence the representation of the transition from the elastic and hardening branch and also the pinching of the hysteretic loops.
- A_3 and A_4, which quantify isotropic hardening.
- For the BLK model the post-yield stiffness (E_h) is the only parameter to be fixed.
- The calibrated material parameters are reported in Table 2, while the comparison of the numerical response and the experimental average envelope is plot in Fig. 3.

3.2.2 Initial camber

It is well known that the sensitivity of the buckling strength to initial camber has practical implications for design and modelling. It was observed that using a camber amplitude arbitrarily selected in the range of 0.05% - 0.1% of brace length may lead to different results. Analyzing the existing literature a large number of existing studies addressed this issue differently. Jin and El-Tawil (2003) utilized an initial imperfection empirically calibrated and equal to 0.2% to simulate the experimental response from shake table test of 0.6 scale three-story X-braced steel frame. In the NIST GCR 10-917-5 guidelines Deierlein *et al*. (2010) indicate initial geometric imperfection amplitude of 0.05 % to 0.1 % of the brace length according to the study provided by Uriz *et al*. (2008). Cho *et al*. (2011) proposed to adjust the width of the initial imperfection on the basis of a trial-and-error procedure in order to match the target buckling strength of the brace. More recently Wijesundara *et al*. (2011) proposed to use an initial camber equal to $L/350$, while Goggins and Salawdeh (2012) proposed to use an initial camber of 1% of the length of the brace. The differences seem to be due to the fact that different types of bracing configurations have been examined in each study. On the other hand theoretical formulations (Maquoi and Rondal 1978, Georgescu 1996, Dicleli and Mehta 2007, Dicleli and Calik 2008) have been also developed to solve this matter.

With the aim to clarify this issue, the influence of the amplitude of Δ_o on the brace response will be investigated and the main results are shown in Section 3.3.2. The out-of-plane imperfections have been calculated using the following formulations:

(1) ECCS (1978). On the basis of Ayrton-Perry theory, the initial deflection is obtained from the condition corresponding to the achievement of the yield stress in the outermost fibre under the combined presence of the buckling load N_b and the related bending moment M (N_b), obtained having assumed an initial sinusoidal shape, thus leading to the following Equation

$$\Delta_0 = \frac{W}{A} \cdot \alpha \cdot \sqrt{\overline{\lambda}^2 - 0.04} \tag{1}$$

being W the section modulus in the buckling plane, A the cross section area, $\bar{\lambda}$ the dimensionless slenderness and α takes into account the element imperfections and characterized the buckling curves adopted in ECCS (1978).

(2) Georgescu (1996). Starting from the same hypotheses, the camber is given by the following

$$\Delta_0 = \left(\frac{1}{x} - 1\right) \cdot \left(1 - \frac{x f_y}{\sigma_E}\right) \cdot \frac{W}{A} \tag{2}$$

where χ is the buckling reduction factor and σ_E is the critical Eulerian stress. The buckling reduction factor can be obtained according to EN 1993:1-1(2005) as function of $\bar{\lambda}$ and α.

(3) EN 1993:1-1 (2005). For structural analysis EN 1993:1-1(2005) recommends to introduce initial local bow imperfections of members in frames sensitive to buckling in a sway mode. The code provides the values of such imperfections in terms of Δ_o/L, where L is the member length.

(4) Dicleli and Mehta (2007). The initial camber Δ_o is derived assuming along the length of the brace a linear variation of the second-order bending moment generated by the axial force in the deflected bi-linear configuration of the strut, by imposing the equilibrium state at the mid-brace the second-order transverse displacement Δ_b of the brace at buckling load N_b. Hence, Δ_o is obtained as follows

$$\Delta_0 = \frac{M_{pb}}{N_b} \cdot \left(1 - \frac{N_b L^2}{12EI}\right) \tag{3}$$

(5) Dicleli and Calik (2008). The initial camber Δ_o is derived assuming that the sinusoidal deformed shape of the brace prior to buckling and the imposing the second order flexural equilibrium in the section located at the mid-length of the buckling semi-wave, Δ_o is obtained as follows

$$\Delta_0 = \frac{M_{pb}}{N_b\left(1 + \frac{N_b L^2}{8EI(\frac{N_b L^2}{\pi^2 EI})}\right)} \tag{4}$$

3.2.3 FB inelasticity element types

Two types of FB inelasticity elements were used, namely the "infrmFB" and "infrmFBPH". The former are formulated to take into account the plasticity along the element, while in the second the inelasticity is concentrating within a fixed length of the element (Scott and Fenves 2006).

Both types of FB elements were examined to highlight the differences in terms of accuracy and computational time.

3.2.4 Number of integration points

This parameter has a key role owing to the fact that the element response is reproduced by integrating the nonlinear uniaxial material response of the individual fibers in which each section has been subdivided, fully accounting for the spread of inelasticity along the member length. In general, the numerical integration of the element integrals may lead to deformation localization at

the end integration points (Coleman and Spacone 2001). In case of material strain hardening negligible localization problems should be expected being necessary a certain number of IPs (Coleman and Spacone 2001). Hence, in order to evaluate the sufficient number of IPs to guarantee accurate integration and to avoid immediate stiffness changes in the response it was examined their effects varying the number from 3 to 10 per element.

3.2.5 Number of elements and shape of the initial camber

In case of FB elements with distributed plasticity the numerical response of straight structural members is not dependant on the number of elements. This is not the case of concentrated plasticity elements, which need calibration of the hinge length changing the length of element. In case of structural elements having curved shape or not-straight axis it is necessary to mesh the model by subdividing the member in a number of FB elements. This is the case of braces simulated imposing a sinusoidal axis as those assumed in some theoretical models (ECCS 1978, Georgescu 1996, Dicleli and Calik 2008). In order to examine the role of both the mesh sizing and the shape of the brace axis, this parameter has been varied from 2 to 32 sub-elements as illustrated in Fig. 4. In addition, this aspect has been investigated for both distributed and concentrated FB elements.

3.2.6 Number of integration fibers

The number of fibers to be used to discretize the element sections is very important to simulate the stress-strain distribution across the element cross-section. The ideal number of section fibers depends on the shape and material characteristics of the latter and on the level of inelastic deformation imposed to the element. A sensitivity study is carried out to establish the optimum number of section fibers. The number of fibers was assigned in the range 10-400.

3.3 Outcomes of parametric analysis

3.3.1 Influence of material model

The results of the analyses carried out to assess the influence of steel model are presented in Fig. 5 with axial force-axial deformation curves. These curves are obtained assuming the camber calculated by Eq. (4), 5 IPs and 100 fibers per element.

It can be observed that the model is capable to predict the typical phases of brace response, namely the buckling, the plastic mechanism with the loss of axial strength, the elastic unloading in compression and the reloading in tension up to the axial yielding.

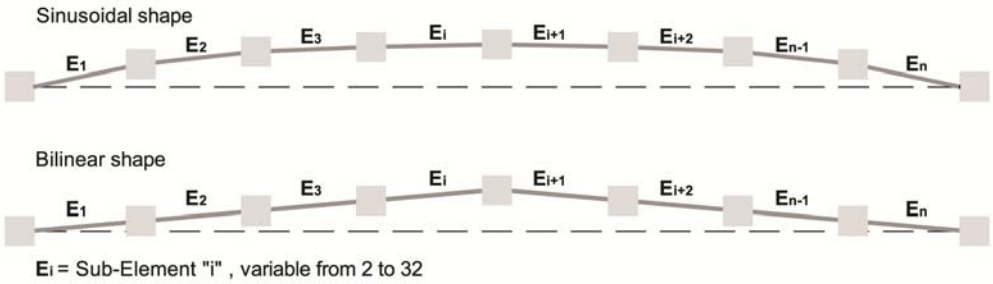

Fig. 4 Discretisation of bracing for both sinusoidal and bilinear shape of the initial camber

The effect of steel model can be observed in the three different phase of brace response that are: (i) the part in large tensile deformation, (ii) the residual post-buckling strength and (iii) the compressive strength and the transition zone beyond the first buckling when the axial compressive load gradually increased up to buckling initiates again.

In tension part the model with steel MP fits well the experimental response, while models with steel BLK slightly underestimates the experimental tensile strength. This result is due to the fact that in BLK the isotropic hardening is neglected. Anyway, for steel BLK the scatter is not significant, being roughly 2% lesser the peak experimental strength.

In residual post-buckling strength the analyses clearly show that the effect of steel model is negligible.

For the camber formulations in Section 3.2.2, both MP and BLK models are able to predict the degradation of the buckling load related to the number of loading cycles as well as the lateral deflection of the brace resulting from the plastic hinge rotations during the previous cycles. Anyway, in the transition zone the models with steel BLK overestimate the buckling strength after the first cycle. As it can be clearly recognized comparing Figs. 5(a) to 5(b) and 5(c), in this phase of the brace response the influence of the material model differs with the type of cross section shape. Indeed, for truss 1 having wide flange section the model with steel BLK give the larger scatter (approximately the 55%) between numerical and experimental values of buckling strength after the first cycle than those given by models with MP (approximately the 32%). In case of braces made of hollow sections (as the case of truss 15 and 17) the models with steel BLK widely overestimated (approximately more than 100%) the compression strength beyond the first buckling, while models with steel MP give an excellent prediction (slightly larger than 5%). These results are due to different reasons. First, BLK model does not take into account the Bauschinger effect, which is characterized by a gradual transition in reloading part of hysteretic loops. In addition, since PTM approach cannot take into account any local buckling phenomena which typically affect the response of hollow sections, a smooth transition from the elastic to the hardening branch of the material stress-strain response allow to compensate fictitiously this lack of the modelling.

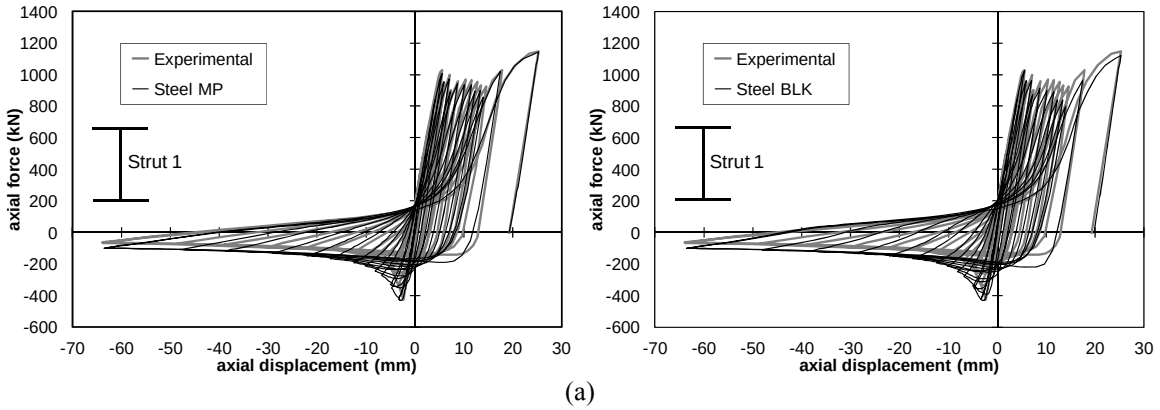

(a)

Fig. 5 Influence of material model: (a) braces having wide flange; (b) circular hollow; and (c) square hollow cross section

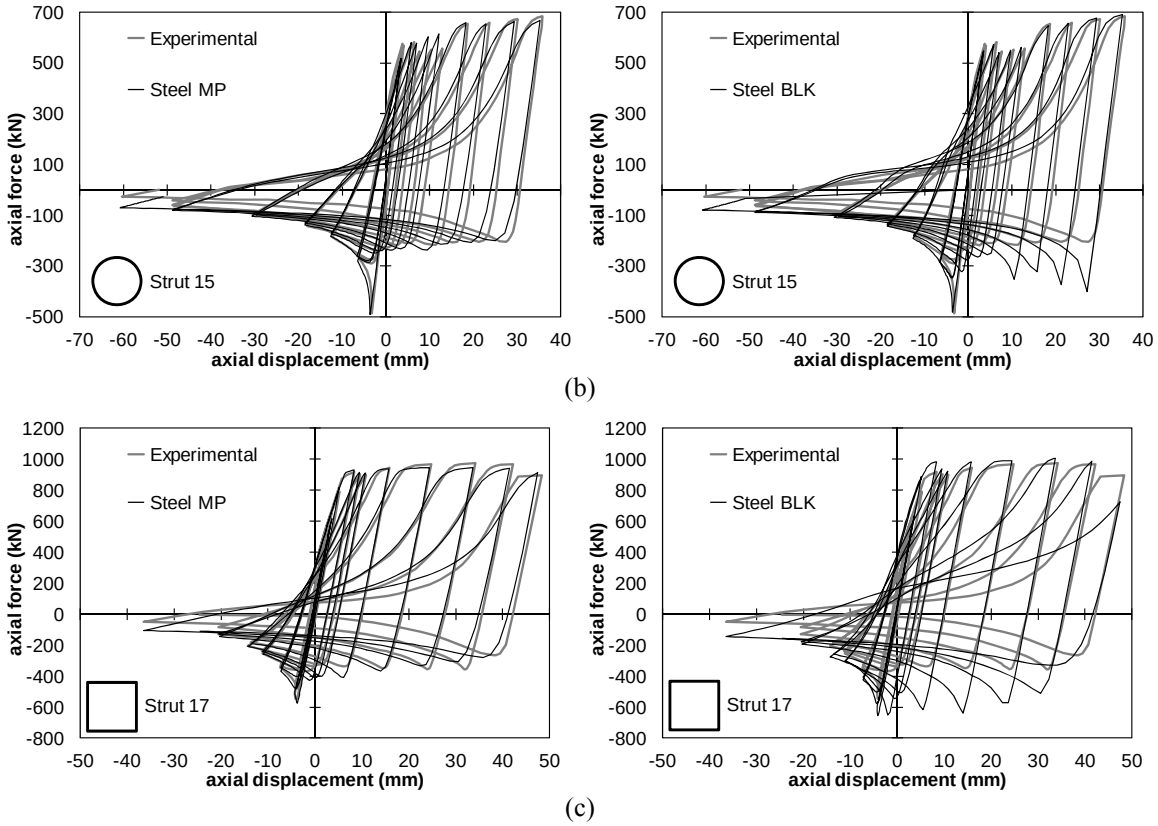

(b)

(c)

Fig. 5 Continued

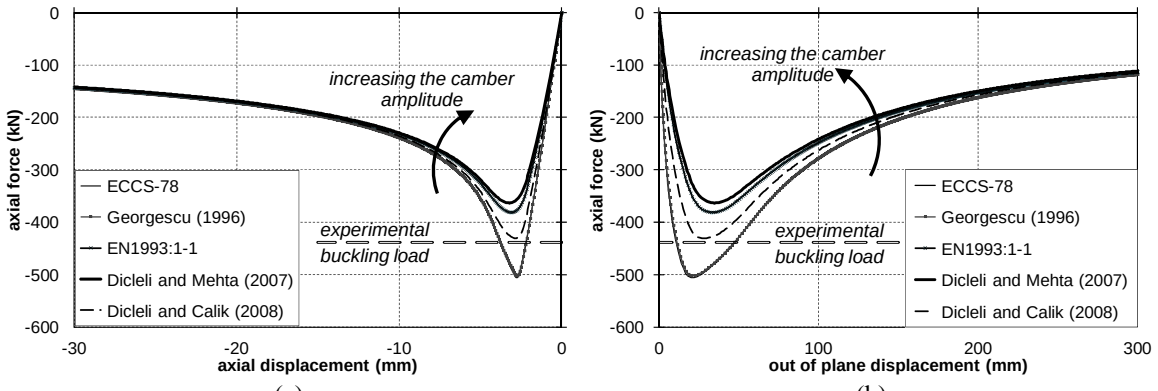

(a) (b)

Fig. 6 Influence of camber under monotonic loading

At the light of the considerations shown in this Section, it can be concluded that the numerical prediction of MP material models matches better the experimental curves. Therefore, the parametric analysis shown hereinafter was carried out using this type of steel model.

3.3.2 Influence of camber

According to the hypotheses of the examined formulations for the camber Δ_o, for these analyses the geometric imperfection was placed where the brace buckled shape experiences the peak transverse displacement. For example, in case of pinned braces the camber was located at 0.5 L.

The strut was initially analyzed under monotonically increasing axial compression displacements. The monotonic response curves in terms of axial force−axial displacement and axial force-lateral deflections for strut 1 are shown in Fig. 6. This plot clearly illustrates the sensitivity of the initial buckling load to the assumed initial camber, where differences in load-carrying capacity diminish as axial displacements increase. As it can be observed, each theoretical formulation gives different amplitudes of initial camber and the value of initial camber varies if the brace section and the brace slenderness change. It should be also noted that the plots depicted in Fig. 6 have been obtained assuming two beam-column elements with distributed plasticity and five IPs each. Increasing the number of sub-elements for each formulation of the camper amplitude leads to a small reduction of the buckling load, but negligible differences in the post-buckling response can be recognized. The influence of the number of sub-elements on the numerical prediction of braces has been deepened in Section 3.3.5.

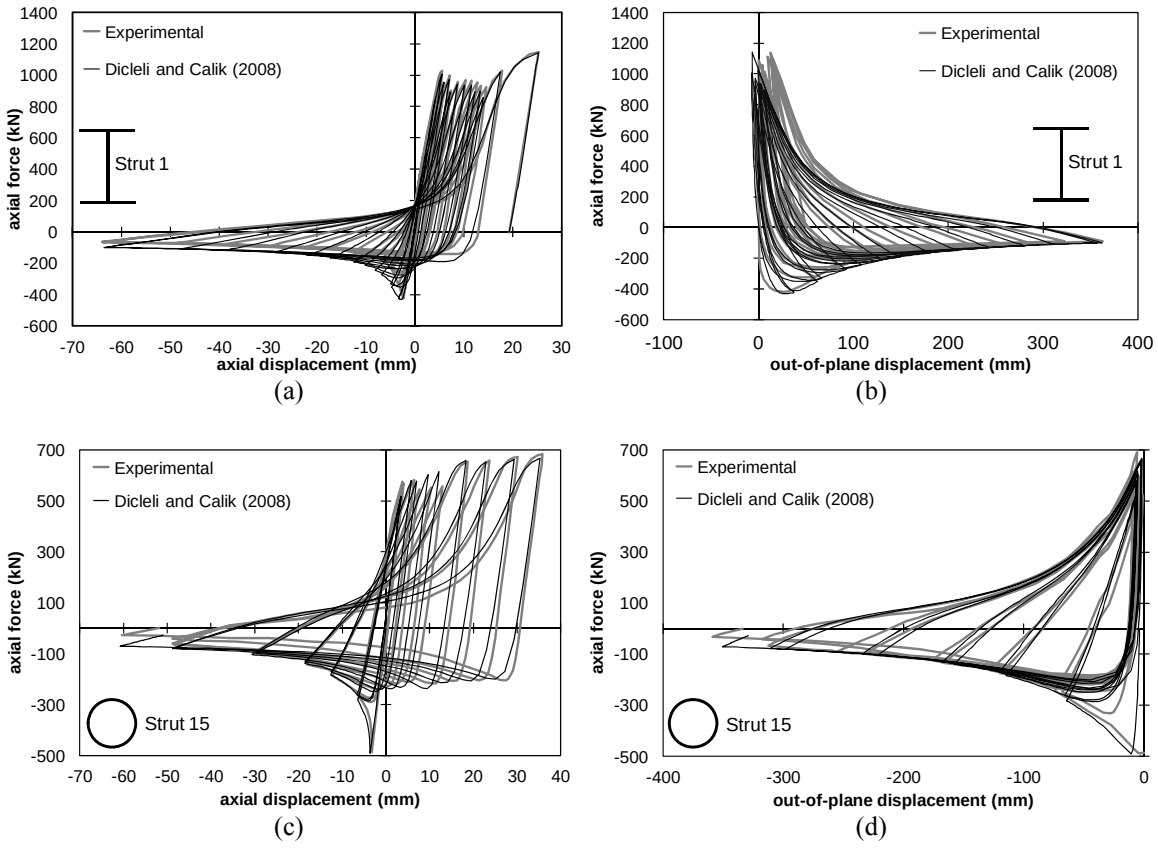

Fig. 7 Accuracy of the models with Dicleli and Calik (2008) formulation under cyclic loading

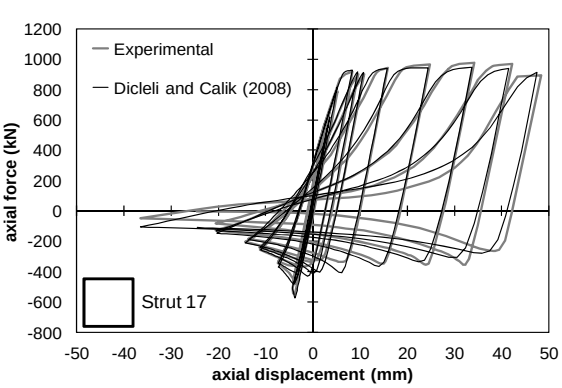

(e)

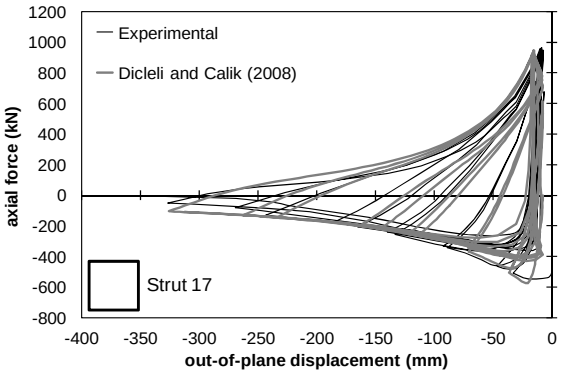

(f)

Fig. 7 Continued

The scatter between numerical and experimental buckling loads and the corresponding statistical parameters (namely mean value, standard deviation "Std.Dev" and coefficient of variation "CV") are reported in Table 3 for each model. As, it can be easily recognized that models with the camber calculated according to Dicleli and Calik (2008) provides the better accuracy to test results.

The influence of camber under cyclic conditions has been also investigated. Also in cyclic conditions the model of Dicleli and Calik (2008) leads to the better resemblance between the test and analysis result (Fig. 7). The results obtained using the other camber formulations lead to a non-negligible misestimate of buckling strength. For all examined formulations the calculated residual post-buckling strength was larger than the experimental value. This outcome highlights one of the limit of PTMs, which is the impossibility to take into account the deterioration phenomena due to the accumulation of plastic deformation in locally buckled parts of plastic hinge zones.

Another important aspect to be highlighted is the influence on the shape and on the area variations of the hysteretic envelopes for each camber formulation and material model, considering the effects on energy absorption. In Table 4 the differences of hysteretic areas (namely dissipated

Table 3 Differences between experimental and numerical buckling load

Strut	*Camber formulation*				
	ECCS-78	Georgescu	EN1993:1-1	Dicleli and Mehta (2007)	Dicleli and Calik (2008)
1	18.56%	17.54%	-10.77%	-14.92%	0.94%
15	1.63%	1.24%	17.06%	10.55%	1.94%
17	14.39%	11.65%	-7.14%	-8.51%	1.03%
Mean	11.53%	10.14%	11.66%	11.33%	1.30%
Std.Dev	8.82%	8.25%	5.02%	3.27%	0.55%
CV	0.77	0.81	0.43	0.29	0.42

Table 4 Differences between experimental and numerical hysteretic envelope areas

Strut	*Steel model*	*Camber formulation*				
		ECCS-78	Georgescu	EN1993:1-1	Dicleli and Mehta (2007)	Dicleli and Calik (2008)
1	MP	4.30%	3.86%	3.19%	3.13%	3.59%
	BLK	9.24%	8.71%	7.55%	7.46%	7.76%
15	MP	4.29%	3.88%	2.93%	1.74%	1.55%
	BLK	23.02%	21.91%	17.37%	10.35%	10.04%
17	MP	5.59%	5.30%	2.70%	1.48%	1.39%
	BLK	30.11%	29.74%	16.61%	15.90%	17.43%

energy) among the examined models is given considering also the influence of the type of steel model. As it can be observed the best approximation to experimental hysteretic areas is given using steel MP.

At the light of the considerations shown in this Section, it can be noted that the better agreements to experimental curves were obtained using the formulation by Dicleli and Calik (2008) and MP material model (Menegotto and Pinto 1973). Therefore, in the following the parametric analysis is shown under these hypotheses.

3.3.3 Distributed vs. concentrated plasticity FB elements

In this Section a comparison of response obtained with distributed and concentrated FB plasticity elements is shown. For concentrated plasticity FB elements the examined plastic hinge lengths range as 10%, 15%, 20%, 25% and 30% of the element length. Referring the strut 1, the monotonic response curves for both concentrated and distributed plasticity elements are depicted in Fig. 8.

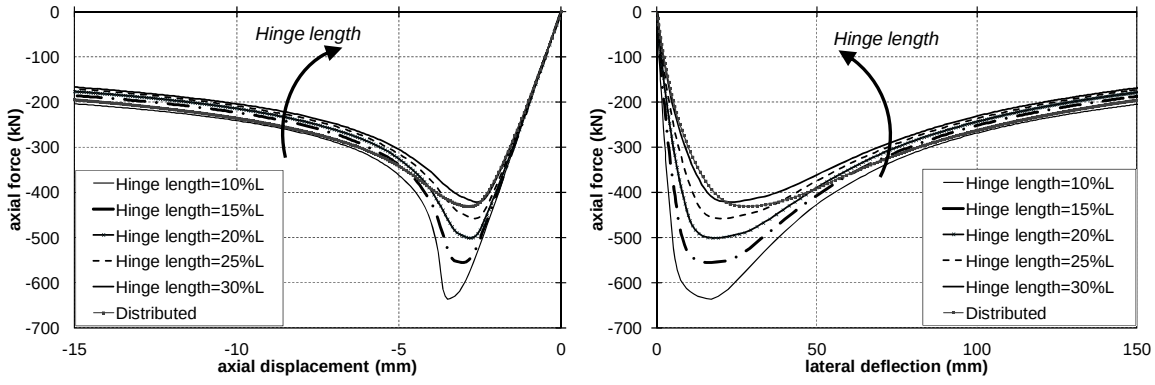

(a) (b)

Fig. 8 Distributed vs. Concentrated FB elements: (a) axial force-axial displacement; (b) axial force-lateral deflection

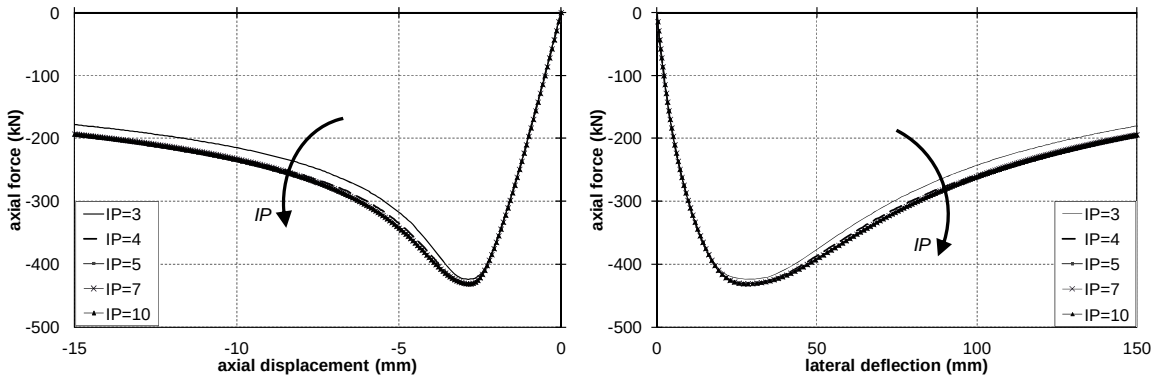

(a) (b)

Fig. 9 Sensitivity to number of IPs: (a) axial force-axial displacement; (b) axial force-lateral deflection

As it can be easily noted, the prediction of buckling load is strongly affected by hinge length. Indeed, if concentrated plasticity elements are used, the reduction of the plastic length produces an increase of strength. For what concerns the transverse displacements, a good agreement for all cases was obtained for high deformation demand. For the case shown the model with plastic hinge equal to 30% L gives the better response as compared to that given by distributed FB elements. Anyway, this result cannot be generalized, since it depends on the length of plastic zone which should be noted a-priori and it varies case by case. Therefore, it is more reliable and effective to use distributed elements, because it is possible to overcome the need to define the plastic hinge length. It is interesting to note that the sensitivity analyses performed varying the type of plasticity element showed that the elapsed time for the analysis with concentrated plasticity elements is lower than in the analysis with distributed plasticity. This is due to the fact that numerical integration of fibers is carried out for the two end sections of the plastic length only.

3.3.4 Influence of number of integration points

Figs. 9(a), (b) show the results for monotonic shortening of the brace varying the number of IPs per element. Owing to under-integration, the model with three IPs per element exhibits the more soften response in the post-buckling regime (about the 8% in the final stage) was recognized. The models with four to ten IPs present similar results, thus highlighting that PTMs of bracing are less affected by localization problems. In addition, it was recognized that reducing the number of IPs leads to minimize the time analysis, but increasing the number of IPs leads to improve the accuracy of the predicted response in nonlinear range.

3.3.5 Influence of the number of elements and of the shape of the initial camber

The analyses showed that increasing the number of distributed plasticity elements in both models with bilinear or sinusoidal shape of the initial camber lead slightly underestimating the brace buckling strength, even though no significant differences can be recognized in post-buckling range, as depicted in Figs. 10(a), (b).

In case of concentrated plasticity elements the computational results are strongly sensitive to the number of sub-elements. As it can be noted in Figs. 10(c), (d) increasing the number of sub-

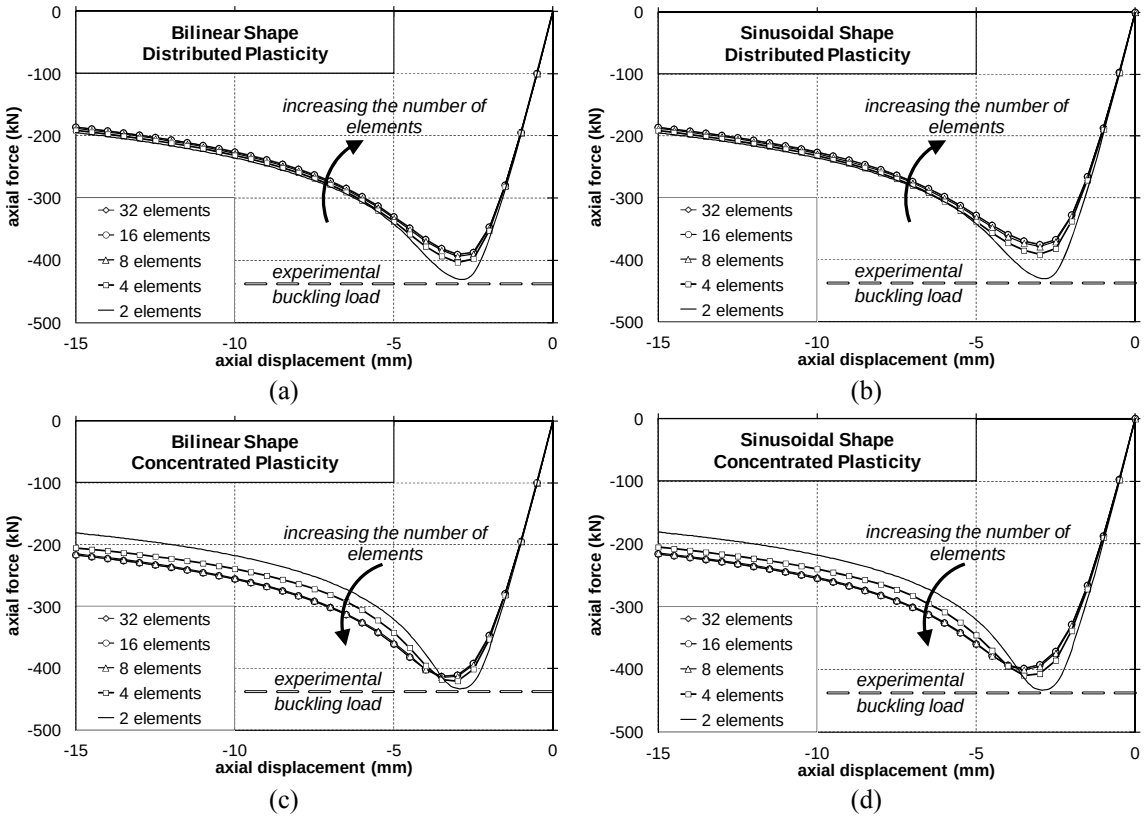

Fig. 10 Sensitivity to number of elements for bilinear and sinusoidal shape of the initial camber

elements does not correspond an improvement of the model predictive response capability. Indeed, a stiffening effect in the descending post-buckling branch can be recognized in both cases with bilinear and sinusoidal shape. As it can be easily foreseen, the computational time is also affected by the number of sub-elements, increasing more than linearly with the number of elements up to 11 times the period elapsed for models with two elements only.

On the basis of these results it can be recognized that the more suitable manner to implement PTMs for bracing is to use distributed plasticity elements with bilinear shape and two elements only, thus providing both sufficient adequate accuracy and reduced computational effort.

3.3.6 Influence of number of fibers

Figs. 11(a), (b) show the results obtained using a number of fibers in cross section varying in the range $10 \div 400$.

As it can be observed the sensitivity to this parameter is small. Only in the case with 10 fibers the hysteretic behaviour and the lateral deflection are not accurately represented. This is due to the reduced flexural stiffness and increased sensitivity to the interaction between moment and axial loads. The case with 25 fibers slightly underestimates the buckling strength, being not enough to represent the interaction between moment and axial loads. This result is mainly related to the numerical integration which determines the second moment of area of brace cross section. Indeed,

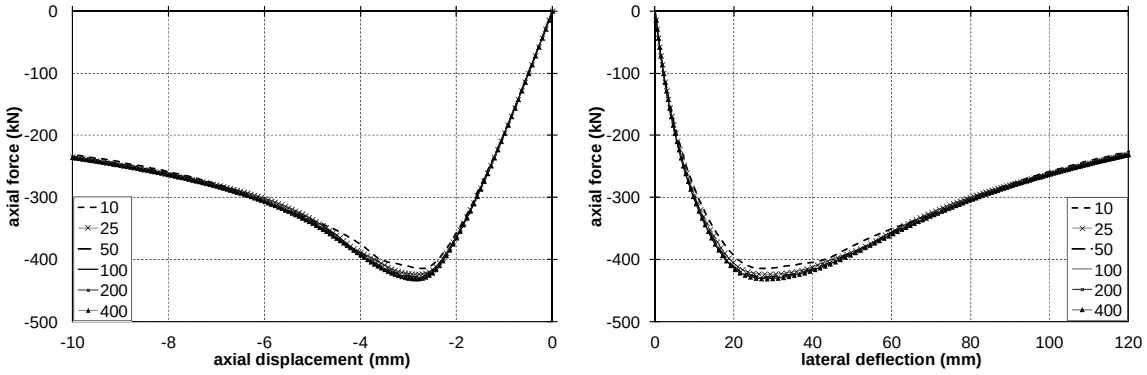

Fig. 11 Sensitivity to number of fibers: (a) axial force-axial displacement; (b) axial force-lateral deflection

as also observed by Uriz (2005) and Salawdeh and Goggins (2013) using fewer fibres to discretize the brace area may lead having lower distance of the centroid for the fibres, thus resulting in a smaller equivalent moment of inertia than that calculated by assuming a larger number of fibres. In addition, the analyses for the examined set of braces showed that some convergence problems may be observed for such a small number of fibers, especially in cases of the presence of biaxial bending moment interaction with axial load.

From 50 to 400 fibers it is observed that the axial hysteretic and monotonic response become independent from the accuracy of the mesh. This result may be explained by the fact that increasing the number of fibers allow to mesh better the section by subdividing the thickness of the plates constituting the cross section. For the examined cases, the analyses showed that it is sufficient to have at least 2 fibers across the thickness to improve the accuracy and the stability of the analysis. In general, increasing the number of fibers makes more stable the computational effort, although it leads increasing the computational time increases. Using 100 fibers with at least two of them across the thickness of the plate components (namely flange, web or walls) is a satisfactory compromise among computational stability and time effort.

4. Nonlinear static analysis of CBFs

4.1 Generality

In order to assess the accuracy of the adopted modelling approach in predicting the nonlinear static response of different braced frame configurations, a X-CBF (Wakawayashi *et al*. 1970) and an inverted V zipper CBF (Yang *et al*. 2008) were analyzed. These bracing configurations were chosen for the complex behaviour if compared to the typical brace schemes used in building.

In particular, for what concerns X-CBFs it is important to analyse the model sensitivity to brace-to-brace interaction, because the brace buckling capacity is influenced by the twin diagonal brace in tension. The case of inverted V zipper CBF is very different, because the presence of tie elements connecting all beams of the braced bays at brace-to-beam intersection points leads all compression braces to buckle simultaneously. This implies that overall instability and collapse can

occur once the full-height zipper mechanism forms, because of the reduced lateral capacity of the frame after a full mechanism has formed.

4.2 Nonlinear static behaviour of X-CBFs

Wakawayashi *et al*. (1970) tested four nominally identical one-storey dual X-braced portal frames, whose geometry is shown in Fig. 12. Different loading conditions were considered for the specimens. In particular, specimens BM0 and BM5 were tested under monotonic pushover, but with different vertical load applied to columns (namely 0 kN and 700 kN, respectively). Specimens BC0 and BC5 were tested under cyclic pushover, but with different vertical load applied to columns (namely 0 kN and 700 kN, respectively).

In the numerical model, full strength and full rigid beam-to-column joints have been considered. Both beam and columns were modelled as distributed plasticity elements with 5 IPs per element and 100 fibers per section, as indicated in Section 3.3.6. The braces have been modelled as perfectly pinned. The restraint effect of the diagonal in tension has been taken into account in the calculation of the geometrical slenderness λ of X-diagonal braces. This effect halves the brace in-plane buckling length, while it is taken as inefficient for out-of-plane buckling. Hence, the geometrical in-plane slenderness has been calculated considering the half brace length, while the out-of-plane ones considering the entire brace length. In this case the in-plane slenderness is maximum and the corresponding camber is calculated with Dicleli and Calik formulation considering the half brace length, thus resulting equal to 0.30% L_o, being L_o the brace buckling length, assumed equal to the length between the brace intersection point and the end working point.

The MP steel has been used for all members, considering for the parameters the values given in Table 2 with the exception of the yield stress (given by experimental tests and equal to 260MPa for columns, 310 MPa for beam and 340 MPa for braces) and post-yield stiffness (equal to 1%).

In monotonic and cyclic analysis, it is applied an incremental horizontal displacement history equal to the experimental protocol.

As shown in Fig. 13, both the monotonic and cyclic performances of the X-CBF specimens have been satisfactorily simulated. Some differences can be recognized at high displacement

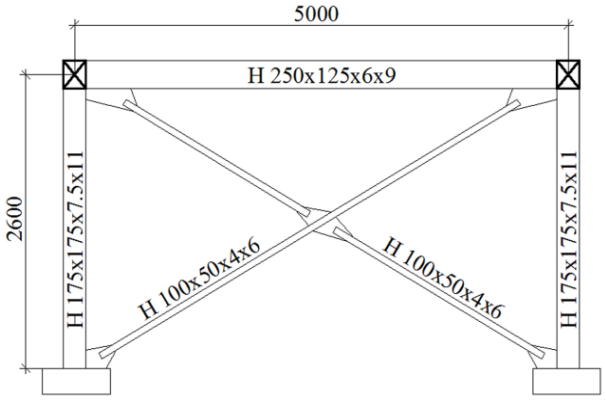

Fig. 12 Geometry of frame tested by Wakawayashi *et al*. (1970)

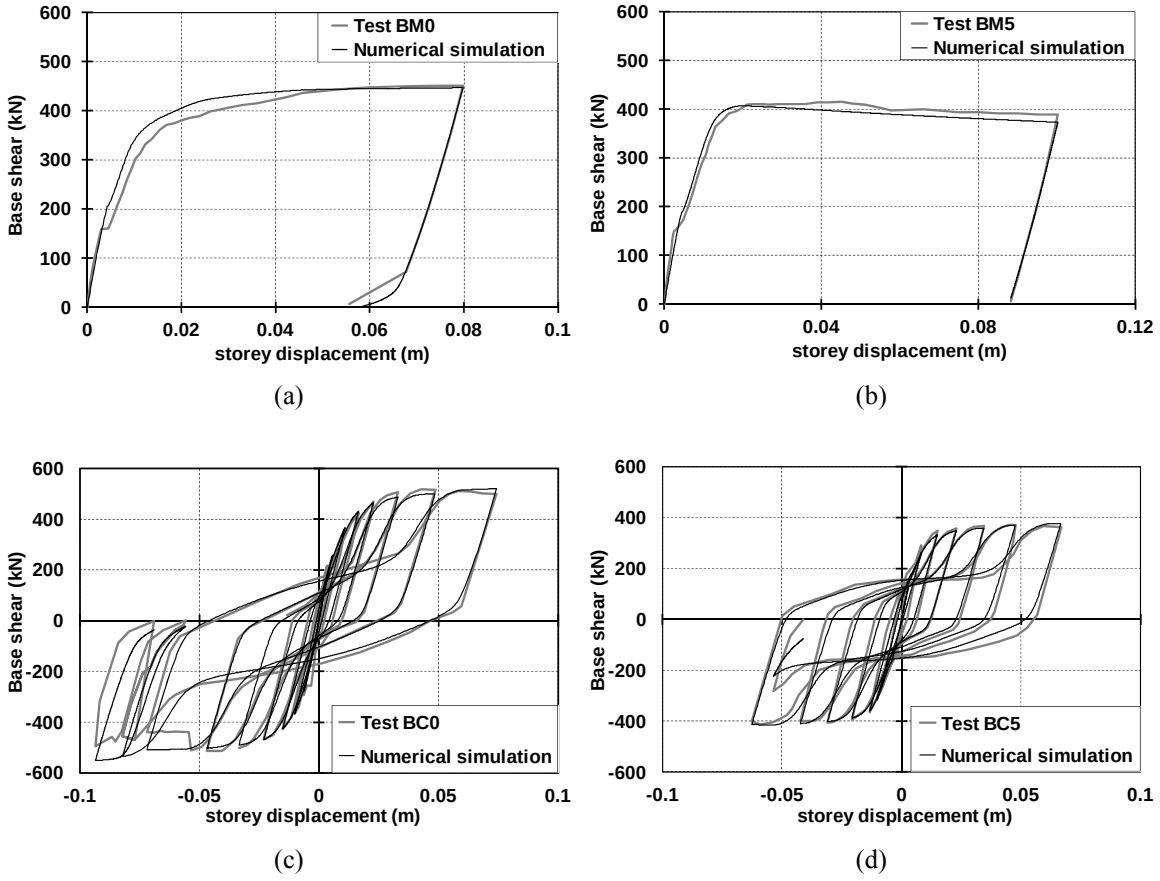

Fig. 13 X-CBFs: numerical vs. experimental response: (a) monotonic; and (b) cyclic condition

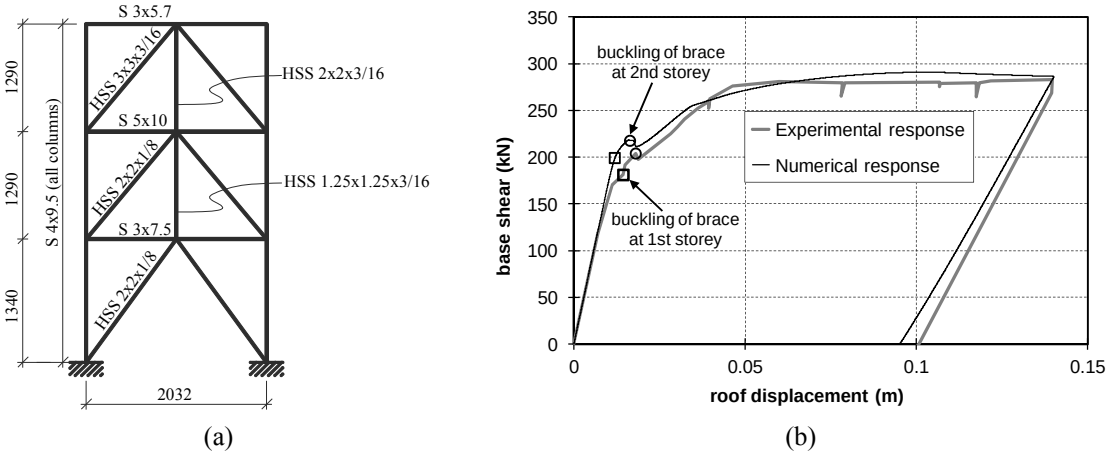

Fig. 14 Frame tested by Yang *et al*. (2008): (a) Geometry; (b) numerical vs. experimental response

demands where some damages in connections were experimentally observed and, as expected, the models cannot reproduce this phenomena.

4.3 Nonlinear static behaviour of inverted V-CBFs with zipper struts

Yang *et al*. (2008) performed a pushover test on a 1/3 scaled model of a 2D zipper frame, which consisted in three storey one zipper braced bay, as shown in Fig. 14(a). The braces and the zipper struts were cold-formed welded and seamless HSS made of ASTM A500 Grade B steel (f_y = 317 MPa and f_u = 400 MPa). The rest of the members were made of A572 Grade 50 (f_y = 345 MPa and f_u = 448 MPa). Gusset plate connections were used for braces and zipper struts, while fully welded column-to-base connections were made in order to obtain fixed restraints. The beam-to-column connections were made to transfer shear and axial forces but not bending moments. However, owing to the considerable in-plane stiffness of the gusset plates connecting the brace, beam and column, the beam end connections can be considered as flexurally rigid restrained.

All elements were modelled as distributed plasticity elements with 5 IPs per element and 100 fibers per section, as indicated in Section 3.3.6. The braces and the zipper struts have been modelled as perfectly pinned. The brace cambers resulted equal to equal to 0.40%, 0.46% and 0.55% of the brace buckling length assumed equal to the length between the working points, as in the previous case. Analogously to the case of X-CBFs, the MP steel has been used for all members.

In pushover analysis, the nodes at each storey are translated horizontally in a series of incremental applied displacements equal to those experimentally applied to the frame specimen.

As depicted in Fig. 14(b), the obtained numerical response strictly matches the experimental curve, reproducing a collapse mode close to that observed in the test. Indeed, the model catches the sequence of brace buckling at first and second storey, which corresponds to the first singularity in the numerical curve.

5. Nonlinear dynamic analysis of CBFs

5.1 Generality

It is well known that the modelling of CBFs in dynamic conditions needs to take into account more aspects than those examined in static loading. In particular, the inertia effects, the equivalent viscous damping and the hysteretic response of nonlinear elements should be carefully addressed, because all of them could significantly affect the dynamic behaviour of the structure. As a consequence, the incorrect modelling of one of them leads to unrealistic and inaccurate numerical outcomes.

Hereinafter, the influence of these aspects on the numerically predicted dynamic response of CBFs has been verified and validated on the basis of a shaking table test carried out by Uang and Bertero (1986).

5.2 Structural details of the investigated frame

The examined structure was a 3D prototype steel concentrically braced building, having six – storeys and a square plan with three frames in the both directions and a composite floor system.

The tested specimen was a reduced-scale prototype from a full-scale building designed according to U.S. Uniform Building Code (UBC) 1979 and Japanese design codes. The size of the prototype was obtained using a scale factor of 0.3048, which complied with the weight, height, and plan limitations of the shaking-table equipments. The model complied with all the material requirements except that of mass density.

In Fig. 15 the building structural plan and elevations are illustrated. All beam-to-column joints of the frames A, B and C in X direction are moment-resisting, while the secondary beams and those belonging to the bays in Y direction are simply pinned. The cross sections of the structural members constituting the experimental mock-up are reported in Table 5.

The structure was subjected to the Miyagi-Ken-Oki, 1978, earthquake (N-S component only) scaled several times. In the present study it is examined the record with P.G.A scaled to 0.33 g.

5.3 FE model

The beams and columns were modelled as distributed plasticity elements with 5 IPs per element and 100 fibers per section, as indicated in Section 3.3.6. All beam-to-column joints were simulated as full strength and full rigid. The braces were modelled as fixed at both ends and the initial camber calculated according to Dicleli and Calik formulation was equal to 0.11% L, being L the length between the brace working points.

The MP steel was used for all members, whose parameters are given by Table 2 with the exception of the yield stress (experimentally obtained and equal to 296 MPa for columns, 317 MPa for beam and 407 MPa for braces) and post-yield stiffness (equal to 1%).

At each floor all nodes are constrained by a rigid in-plane diaphragm allowing having only three dynamic degrees of freedom at each floor, i.e. two translations and one torsional rotation.

The acceleration input is applied in X direction (see Fig. 15(a)) to all nodes at the basis of the model, which correspond to those physically attached to the shake table platform. The numerical response is calculated using the Newmark numerical integration scheme with a time-step of 0.005 sec and internal iterations within each time-step.

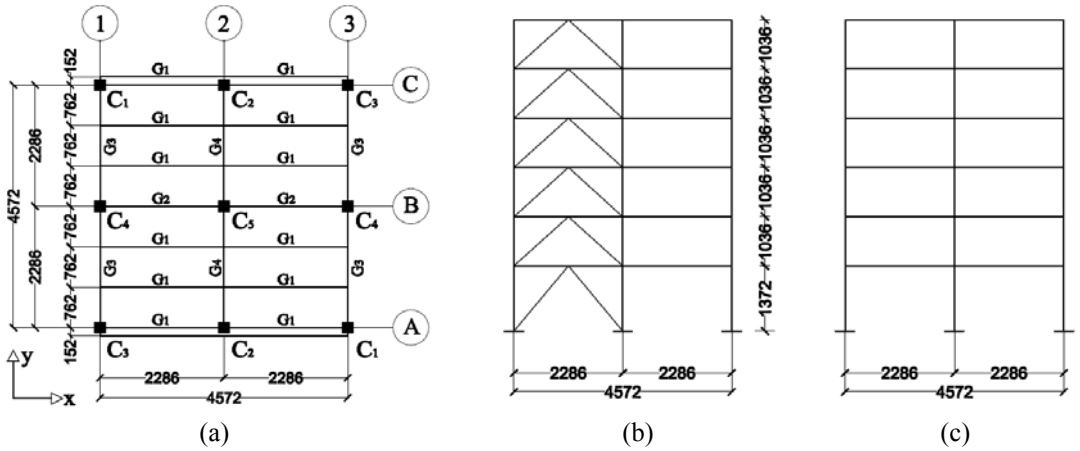

(a) (b) (c)

Fig. 15 Test Uang and Bertero (1986): (a) the building structural plan; (b) the elevation frame B; and (c) elevation frame 1-2-3-A-C

Table 5 Cross sections of steel members of the mock-up tested by Uang and Bertero (1986)

	Girders (*)				Columns (*)					Brace
Storey	G_1	G_2	G_3	G_4	C_1	C_2	C_3	C_4	C_5	
(-)	(-)	(-)	(-)	(-)	(-)	(-)	(-)	(-)	(-)	(-)
6	16W31	16W31	18W35	21W50	10W33	10W33	10W49	10W33	12W40	$4 \times 4 \times 1 / 5.56$
5	16W31	16W31			10W33	10W33	10W49	10W33	12W40	$5 \times 5 \times 1 / 5.56$
4	16W31	18W35			10W39	12W53	12W65	10W60	12W72	$6 \times 6 \times 1 / 4$
3	18W35	18W35			10W39	12W53	12W65	10W60	12W72	$6 \times 6 \times 1 / 4$
2	18W35	18W40			12W50	12W65	12W79	12W79	12W106	$6 \times 6 \times 1 / 4$
1	18W40	18W40			12W65	12W87	12W87	12W106	12W136	$6 \times 6 \times 1 / 2$

(*) see Fig. 15(a)

Table 6 Experimental vs. numerical fundamental periods of vibration

	T_1 (s)	$(T_{1,num}-T_{1,exp})/T_{1,exp}$	T_2 (s)	$(T_{2,num}-T_{1,exp})/T_{1,exp}$	T_3 (s)	$(T_{1,num}-T_{1,exp})/T_{1,exp}$
experimental test (*)	0.365		0.126		0.071	
distributed mass	0.354	– 3.11%	0.127	1.20%	0.072	1.59%
lumped mass	0.344	– 5.85%	0.124	– 1.20%	0.070	– 1.23%

(*) average fundamental periods of vibration have been measured by Uang and Bertero (1986)

5.4 Influence of inertia modelling

In order to investigate the sensitivity to the inertia modelling, the masses were applied to the model in two different approaches, as follows:

- The masses are distributed along each elements, namely applied by magnifying the self masses of each horizontal element up to the total mass corresponding to the relevant tributary area;
- Masses are lumped at the centroid of inertias at each floor, namely the material models constituting the elements are simulated without mass.

As reported in Table 6, the eigenvalue analysis showed that both approaches allow a good modelling of the inertia characteristics. Anyway, the former approach matches better the first period of vibration experimentally measured. Since the first mode dominates the dynamic response, having in this case a participating mass equal to 79% of total mass, the first approach is used in the following.

5.5 Influence of equivalent viscous damping

It is well known that to perform a nonlinear time-history analysis elastic damping should be specified in order to take into account the damping forces in the initial stages before the structural damage. The level of initial damping is normally specified as a percentage of critical damping, which is typically assumed equal to 5% for reinforced concrete structures and 2% for steel structures.

Two different formulations of the Rayleigh damping were investigated and discussed in order

to assess the influence of the level of initial damping on the activation of hysteretic damping due to the structural damage in inelastic time-history analysis. The first formulation relates the damping to the initial elastic stiffness matrix, this implies that the damping coefficient is constant during the analysis, even in the inelastic range of structural response. The second type is relating the damping to the tangent stiffness matrix, where the damping coefficient is proportional to the instantaneous value of the structure stiffness matrix and it is updated when the stiffness matrix changes. Anyway, in both cases it is necessary to define initial damping values, specified as a percentage of critical damping, for the first and last mode of interest, which are modes 1 and 2 in the present case. Those experimentally measured were equal to 1.89 % (standard deviation = 0.366 and coefficient of variation = 19.39%) for mode 1 and 1.93 % (standard deviation = 0.624 and coefficient of variation = 32.35%) for mode 2. For sake of simplicity, being also consistent with the value typically assumed for steel structures, an elastic damping ratio equal to 2% for mode 1 and 2 was used.

In Fig. 16 the response curves using initial and tangential stiffness damping are compared in terms of interstorey drift ratios at the 2nd and 5th floor where the braces buckle. As it can be observed using initial-stiffness elastic damping lead to displacement demands smaller than 30% of those obtained using tangent stiffness damping. This result confirmed what early observed in case of reinforce concrete structures by (Priestley and Grant 2005, Charney 2008). Indeed, using initial stiffness damping leads to large spurious damping forces when the structure gets into inelastic field. Indeed, the artificial damping forces are numerically given by the product of the post-event velocities of deformation multiplied by the initial stiffness and by the stiffness proportional damping constant (Charney 2008), being larger at high ductility demand and when hysteretic energy is low, which is the case of CBFs. The use of tangential stiffness damping does not produce this artificial damping.

In the opinion of the authors, this aspect is very important, because the vast majority of previous researches on seismic analysis of CBFs have been carried out using initial stiffness damping. On the other hand, the most of existing commercial and research software still use Rayleigh damping with initial stiffness damping.

In Fig. 17 the comparison of experimental curves and the numerical response obtained with

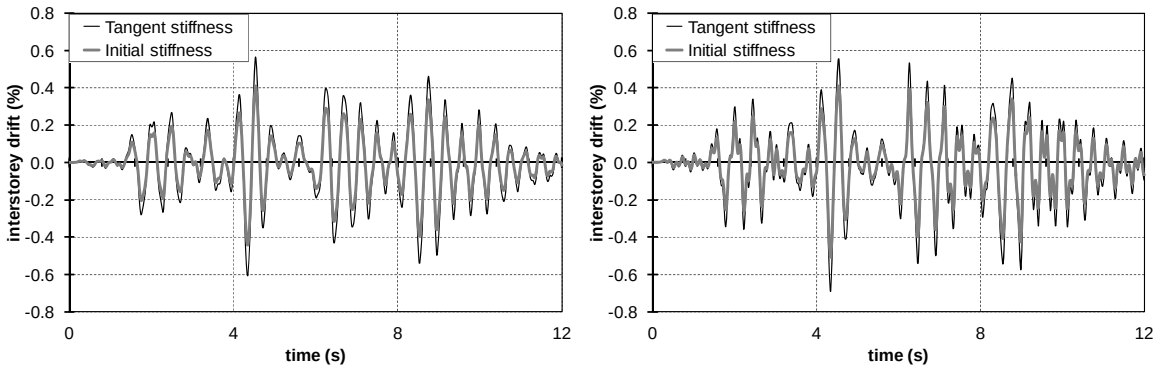

(a) (b)

Fig. 16 Initial vs tangent stiffness damping: (a) 2nd floor; (b) 5th floor

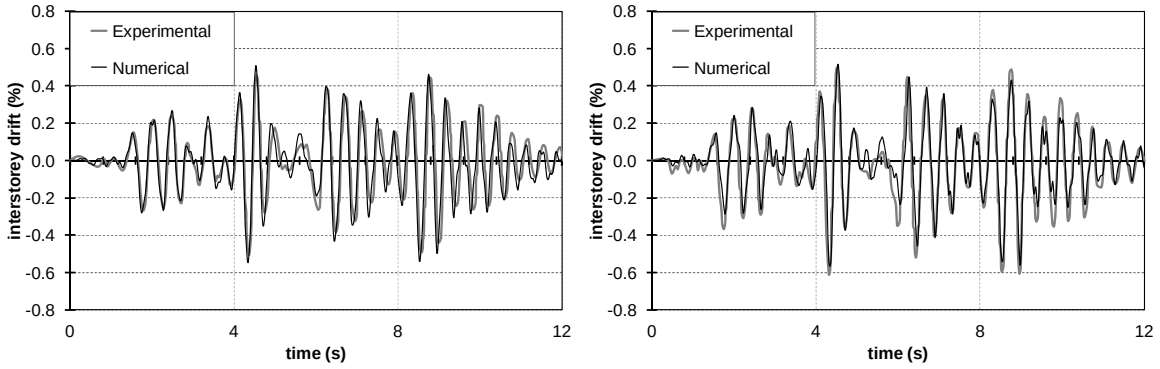

Fig. 17 Experimental vs. numerical interstorey drift (model with tangent stiffness damping): (a) 2nd floor; (b) 5th floor

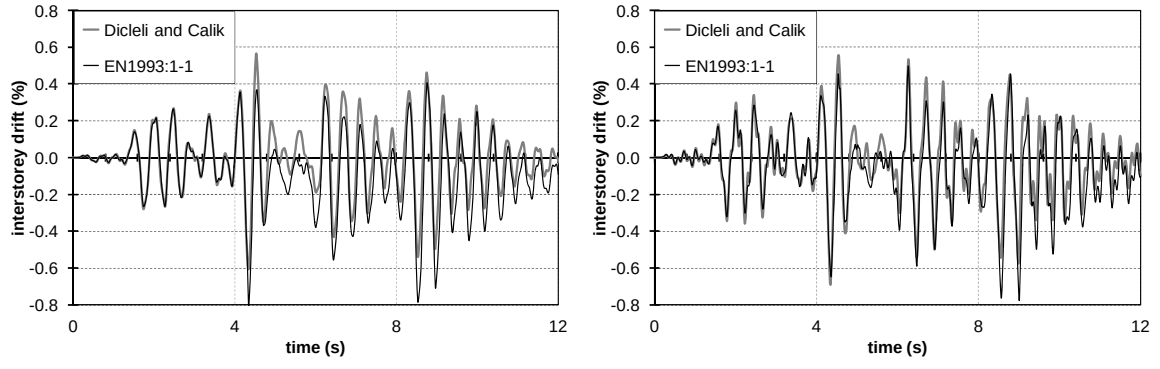

Fig. 18 Influence of initial camber on the dynamic response: (a) 2nd floor; (b) 5th floor

tangent stiffness damping clearly highlights that the best prediction of displacement response isgiven by the tangential stiffness elastic damping, particularly up to $T = 9.4$ sec, where the buckling at 2nd and 5th storey occurred. After this time step the residual displacements are slightly underestimated.

5.6 Influence of brace camber

The correct definition of brace camber is even more important in dynamic analysis than in static conditions, because the amplitude of camber affects the numerical hysteretic behaviour and consequently the hysteretic damping. In order to show the sensitivity of CBF inelastic dynamic response on brace camber in Fig. 18, it is depicted the comparison between the numerical response obtained with camber by Dicleli and Calik (2008) and the one obtained with camber by EN 1993:1-1 (2005). As it can be easily recognized the latter model widely missed the prediction of displacements. This is due to the larger value of brace camber (= 0.20 L) thus leading to anticipate

the brace buckling. Hence, the larger is the brace camber and the larger is stiffness decrease, resulting in larger damage concentration and residual drifts.

6. Conclusions

The main issues related to the numerical modelling for seismic analyses of steel concentric braced frames were highlighted and discussed.

Physical-theory models (PTMs) of braces were implemented using force-based (FB) elements with distributed or concentrated inelasticity and fibre discretization of the cross section. The features of the nonlinear finite element based software Seismostruct were adopted.

The accuracy of numerical prediction obtained using different assumptions for modelling parameters proposed in the literature is examined, extending the analysis to structural configurations and loading conditions different from those used for validation in the relevant original studies, considering the monotonic and cyclic response of braced structures under pseudo-static and dynamic loading conditions.

The examined parameters are the initial camber to trigger brace buckling, the type of material model, the type of force-based element, the number of integration points and the number of fibers to discretize the cross section.

On the basis of numerical investigation on a set of different struts experimentally tested by Black *et al*. (1980), the following considerations can be drawn;

(1) the brace member should be subdivided into two FB distributed plasticity elements with a number of integrating section larger than 4.
(2) the amplitude of initial camber calculated according to Dicleli and Calik (2008) gives the better accuracy.
(3) the model of Menegotto and Pinto (1973) should be used to simulate the material model.
(4) the cross section should be meshed with 100 fibers and at least two of them across the thickness of the plate components (namely flange, web or walls).

Once examined the response of single brace, the modelling aspects of whole braced structures were investigated, as well. The effectiveness of the proposed modelling recommendations was verified in nonlinear static field for different type of bracing systems tested in literature (Wakawayashi *et al*. 1970, Yang *et al*. 2008, Uang and Bertero 1986). These configurations were selected to test the model sensitivity to brace-to-brace interaction in X-CBFs and to verify the versatility of the model also on more complex configuration as the case of inverted V zipper CBF. The comparison between numerical and experimental response curve showed an excellent agreement.

Finally, the aspects related to the numerical modelling of CBFs in nonlinear dynamic conditions were investigated. The effectiveness of numerical results was verified on the basis of shaking table tests taken from literature.

The influence of brace camber on the inelastic dynamic response was investigated. The amplitude of camber affects the numerical hysteretic behaviour and consequently the hysteretic damping, thus leading to miss the displacement demand and the residual drifts. Hence, it is crucial to calculate appropriately the entity of initial imperfection.

Comparing the numerical curves to those experimentally obtained, it was observed that initial stiffness elastic damping can lead to underestimate the displacement demand owing to the presence of large artificial damping forces when the structure enters in the inelastic range. On the

contrary, the use of tangent stiffness damping is most appropriate, because it gives an excellent prediction of displacement response.

Acknowledgements

The financial support of HSS-SERF project (No. RFSR-CT-2009-00024) is gratefully acknowledged.

References

Abramowitz, M. and Stegun, I.A. (1964), *Handbook of Mathematical Functions*, National Bureau of Standards, Applied Math. Series, Vol. 55.

Archambault, M.H., Tremblay, R. and Filiatrault, A. (1995), *Etude du Comportement Seismique des Contreventements Ductiles en X avec Profile's Tubulaires en Acier*, Rapport No. EPM/GCS-1995-09, In: Montreal, Canada: Departement de Genie Civil, Ecole Polytechnique. [In French]

Black, G.R., Wenger, B.A. and Popov, E.P. (1980), *Inelastic Buckling of Steel Struts Under Cyclic Load Reversals*, *UCB/EERC-80/40*, Earthquake Engineering Research Center, Berkeley, CA, USA.

Calabrese, A., Almeida, J.P. and Pinho, R. (2010), "Numerical issues in distributed inelasticity modelling of RC frame elements for seismic analysis", *J. Earthq. Eng.*, **14**(1), 38-68.

CEN (2005), "Eurocode 3: Design of steel structures – Part 1: General rules and rules for buildings, EN 1993-1 1", European Committee for Standardisation, Brussels, Belgium.

CEN (2005), "Eurocode 8: Design of structures for earthquake resistance – Part 1: General rules, seismic actions and rules for buildings, EN 1998-1", European Committee for Standardisation, Brussels, Belgium.

Charney, F.A. (2008), "Unintended consequences of modeling damping in structures", *J. Struct. Eng. ASCE*, **134**(4), 581-592.

Cho, C.H., Lee, C.H. and Kim, J.J. (2011), "Prediction of column axial forces in inverted V-braced seismic steel frames considering brace buckling", *J. Struct. Eng. ASCE*, **137**(12), 1440-1450.

Coleman, J. and Spacone, E. (2001), "Localization issues in force-based frame elements", *J. Struct. Eng. ASCE*, **127**(11), 1257-1265.

Correia, A.A. and Virtuoso, F.B.E. (2006), "Nonlinear analysis of space frames", *Proceedings of the Third European Conference on Computational Mechanics*: *Solids*, *Structures and Coupled Problems in Engineering*, (Mota Soares *et al*. Eds.), Lisbon, Portugal.

D'Aniello, M., Della Corte, G. and Mazzolani, F.M. (2006a), "Seismic upgrading of RC buildings by buckling restrained braces: Experimental results vs numerical modeling", *Proceedings of the 5th International Conference on Behaviour of Steel Structures in Seismic Areas – Stessa 2006*, Yokohama, August, 815-820.

D'Aniello, M., Della Corte, G. and Mazzolani, F.M. (2006b), "Seismic upgrading of RC buildings by steel eccentric braces: Experimental results vs numerical modeling", *Proceedings of the 5th International Conference on Behaviour of Steel Structures in Seismic Areas – Stessa 2006*, Yokohama, August, 809-814.

D'Aniello, M., Della Corte, G. and Mazzolani, F.M. (2008), "Experimental tests of a real building seismically retrofitted by special Buckling-Restrained Braces", *AIP Conference Proceedings 1020* (*PART 1*), Reggio Calabria, July, 1513-1520.

D'Aniello, M., Portioli, F. and Landolfo, R. (2010), "Modelling issues of steel braces under extreme cyclic actions", *COST ACTION C26*: *Urban Habitat Constructions under Catastrophic Events – Proceedings of the Final Conference*, Naples, September.

Deierlein, G.G., Reinhorn, A.M. and Willford, M.R. (2010), *Nonlinear Structural Analysis for Seismic Design: A Guide for Practicing Engineers*, NIST GCR 10-917-5, National Institute of Standards and

Technology, CA, USA.
Della Corte, G., D'Aniello, M. and Landolfo, R. (2013), "Analytical and numerical study of plastic overstrength of shear links", *J. Constr. Steel Res.*, **82**, 19-32.
Dicleli, M. and Calik, E.E. (2008), "Physical theory hysteretic model for steel braces", *J. Struct. Eng. ASCE*, **134**(7), 1215-1228.
Dicleli, M. and Mehta, A. (2007), "Simulation of inelastic cyclic buckling behavior of steel box sections", *Comput. Struct.*, **85**(7-8), 446-457.
ECCS (1978), *European Recommendations for Steel Construction*, European Convention for Constructional Steelwork, (Sfintesco, D.), Brussels, Belgium.
Fell, B.V., Kanvinde, A.M., Deierlein, G.G. and Myers, A.T. (2009), "Experimental investigation of inelastic cyclic buckling and fracture of steel braces", *J. Struct. Eng. ASCE*, **135**(1), 19-32.
Filippou, F.C. and Fenves, G.L. (2004), "Methods of analysis for earthquake-resistant", Chapter 6 from *Engineering Seismology to Performance-Based Engineering*, (Bozorgnia, Y. and Bertero, V.V. eds.), CRC Press, FL, USA.
Filippou, F.C., Popov, E.P. and Bertero, V.V. (1983), *Effects of Bond Deterioration on Hysteretic Behavior of Reinforced Concrete Joints*, EERC Report 83-19, Earthquake Engineering, Research Center, Berkeley, CA, USA.
Fragiadakis, M. and Papadrakakis, M. (2008), "Modeling, analysis and reliability of seismically excited structures: Computational issues", *Int. J. Comput. Methods*, **5**(4), 483-511.
Georgescu, D. (1996), "Earthquake-recent developments in theoretical and experimental results on steel structures. Seismic resistant braced frames", *Costruzioni metalliche*, **1**, 39-52.
Goggins, J.M., Broderick, B.M., Elghazouli, A.Y. and Lucas, A.S. (2006), "Behavior of tubular steel members under cyclic axial loading", *J. Constr. Steel Res.*, **621**(2), 121-131.
Goggins, J.M., Broderick, B.M. and Elghazouli, A.Y. (2008), "Earthquake testing and response analysis of concentrically-braced sub-frames", *J. Constr. Steel Res.*, **64**(9), 997-1007.
Goggins, J. and Salawdeh, S. (2012), "Validation of nonlinear time history analysis models for single-storey concentrically braced frames using full-scale shake table tests", *Earthq. Eng. Struct. Dyn.*, DOI: 10.1002/eqe.2264. [In press]
Ikeda, K. and Mahin, S.A. (1986), "Cyclic response of steel braces", *J. Struct. Eng. ASCE*, **112**(2), 342-361.
Jain, A.K. and Goel, S. (1978), *Hysteresis Models for Steel Members Subjected to Cyclic Buckling or Cyclic End Moments and Buckling-Users Guide for DRAIN-2D*, University of Michigan, College of Engineering, Ann Arbor, MI, USA
Jin, J. and El-Tawil, S. (2003), "Inelastic cyclic model for steel braces", *J. Eng. Mech. ASCE*, **129**(5), 548-557.
Lee, S. and Goel, S.C. (1987), *Seismic Behavior of Hollow and Concrete-Filled Square Tubular Bracing Members*, Research Rep. No. UMCE 87-11, University of Michigan, Ann Arbor, MI, USA.
Lee, P.S and Noh, C.H. (2010), "Inelastic buckling behavior of steel members under reversed cyclic loading", *Eng. Struct.*, **32**(9), 2579-2595.
Maquoi, R. and Rondal, J. (1978), "Mise en équation des nouvelles courbes européennes de flambement", *Construction Métallique*, **1**, 17-30. [In French]
Mazzolani, F.M., Della Corte, G. and D'Aniello, M. (2009), "Experimental analysis of steel dissipative bracing systems for seismic upgrading", *J. Civ. Eng. Manag.*, **15**(1), 7-19.
Menegotto, M. and Pinto, P.E. (1973), "Method of analysis for cyclically loaded reinforced concrete plane frames including changes in geometry and non-elastic behavior of elements under combined normal Force and bending", *Proceedings IABSE Symposium on Resistance and Ultimate Deformability of Structures Acted on by Well Defined Repeated Loads*, Lisbon, Portugal.
Nip, K.H., Gardner, L. and Elghazouli, A.Y. (2010), "Cyclic testing and numerical modelling of carbon steel and stainless steel tubular bracing members", *Eng. Struct.*, **32**(2), 424-441.
Priestley, M.J.N. and Grant, D.N. (2005), "Viscous damping in seismic design and analysis", *J. Earthq. Eng.*, **9**(1), 229-255.
Salawdeh, S. and Goggins, J. (2013), "Numerical simulation for steel brace members incorporating a fatigue

model", *Eng. Struct.*, **46**, 332-349.
Scott, M.H. and Fenves, G.L. (2006), "Plastic hinge integration methods for force-based beam–column elements", *J. Struct. Eng. ASCE*, **132**(2), 244-252.
Seismosoft (2011), "SeismoStruct – A computer program for static and dynamic nonlinear analysis of framed structures", Available from URL: www.seismosoft.com
Serra, M., Rebelo, C., Silva, L.S., Tenchini, A., D'Aniello, M. and Landolfo, R. (2012), "Study on concentrically V-braced frames under cyclic loading", *Proceedings of Stessa 2012 Conference*, Santiago, Chile, January.
Shaback, B. and Brown, T. (2003), "Behavior of square hollow structural steel braces with end connections under reversed cyclic axial loading", *Can. J. Civ. Eng.*, **30**(4), 745-753.
Shibata, M. (1982), "Analysis of elastic-plastic behavior of a steel brace subjected to repeated axial force", *Int. J. Solids Struct.*, **18**(3), 217-228.
Spacone, E., Ciampi, V. and Filippou, F.C. (1996), "Mixed formulation of nonlinear beam finite element", *Comput. Struct.*, **58**(I), 71-83.
Szabó, B.A. and Babuška, I. (1991), *Finite Element Analysis*, John Wiley & Sons.
Takeuchi, T. and Matsui, R. (2011), "Cumulative cyclic deformation capacity of circular tubular braces under local buckling", *J. Struct. Eng. ASCE*, **137**(11), 1311-1318.
Tang, X. and Goel, S.C. (1989), "Brace fractures and analysis of phase I structures", *J. Struct. Eng. ASCE*, **115**(8), 1960-1976.
Tremblay, R. (2002), "Inelastic seismic response of steel bracing members", *J. Constr. Steel Res.*, **58**(5-8), 665-701.
Tremblay, R., Archambault, M.H. and Filiatrault, A. (2003), "Seismic response of concentrically brace steel frames made with rectangular hollow bracing members", *J. Struct. Eng. ASCE*, **129**(12), 1626-1636.
Uang, C.M. and Bertero, V.V. (1986), *Earthquake Simulation Tests and Associated Studies of a 0.3-Scale Model of a Six-Story Concentrically Braced Steel Structure*, University of California, Berkeley, CA, USA.
Uriz, P. (2005), "Towards earthquake resistant design of concentrically braced steel buildings", Ph.D. Dissertation, Department of Civil and Environmental Engineering, University of California, Berkeley, CA, USA.
Uriz, P., Filippou F.C. and Mahin, S.A. (2008), "Model for cyclic inelastic buckling of steel braces", *J. Struct. Eng. ASCE*, **134**(4), 619-628.
Wakawayashi, M., Matsui, C., Minami, K. and Mitani, I. (1970), *Inelastic Behaviour of Full Scale Steel Frames*, Kyoto University Research Information Repository, Disaster Prevention Research Institute annuals.
Wijesundara, K.K. (2009), "Design of concentrically braced steel frames with RHS shape braces", Ph.D. Dissertation, Pavia: European Centre for Training and Research in Earthquake Engineering (EUCENTRE).
Wijesundara, K.K., Nascimbene, R. and Sullivan, T.J. (2011), "Equivalent viscous damping for steel concentrically braced frame structures", *B. Earthq. Eng.*, **9**(5), 1535-1558.
Yang, C.S., Leon, R.T. and DesRoches, R. (2008), "Pushover response of a braced frame with suspended zipper struts", *J. Struct. Eng. ASCE*, **134**(10), 1619-1626.

CC